METRICA
METRology Institutional CAtalog

ISTITUTO NAZIONALE DI RICERCA METROLOGICA
Repository Istituzionale

The Measurement of the Silicon Lattice Parameter and the Count of Atoms to Realise the Kilogram

(Article begins on next page)

24 April 2024

The Measurement of the Silicon Lattice Parameter and the Count of Atoms to Realise the Kilogram

Enrico Massa, Carlo Paolo Sasso & Giovanni Mana

ONLINE FIRST

🨩 Springer

Springer

Check for
updates

ORIGINAL PAPER

The Measurement of the Silicon Lattice Parameter and the Count of Atoms to Realise the Kilogram

E. Massa* , C. P. Sasso and G. Mana

INRIM - Istituto Nazionale di Ricerca Metrologica, Strada delle Cacce 91, 10135 Turin, Italy

© The Author(s) 2020

Abstract: X-ray interferometry established a link between atomic and macroscopic realisations of the metre. The possibility of measuring the silicon lattice parameter in terms of optical wavelengths opened the way to count atoms, to determine the Avogadro constant with unprecedented accuracy, and, nowadays, to realise the kilogram from the Planck constant. Also, it is a powerful tool in phase-contrast imaging by X-rays and, combined with optical interferometry, in linear and angular metrology with capabilities at the atomic scale. This review tells the history of the development of this fascinating technology at the Istituto Nazionale di Ricerca Metrologica in the last forty years. Eventually, it highlights its contribution to the redefinition of the International System of Units (SI).

Keywords: International system of units; Avogadro constant; Planck constant; Silicon lattice parameter; X-ray interferometry

1. Introduction

In 1963, Egidi [1] figured a natural mass standard realised by counting the atoms in a crystal, "scaled so to result outside in the form of a cube with faces parallel to the reticular planes". He stated that the crystal should be prepared with a mass near to 1 kg and should be a mononuclidic element, with impurities not exceeding 0.1 nmol/mol and dislocations or other defects not exceeding a similar concentration. Also, he anticipated that the distance between the crystal's lattice planes and its outer dimensions should be measured to within a 0.1 nm/m fractional accuracy.

Two years later, Bonse and Hart [2] paved the way to accurate measurements of the silicon lattice parameter by operating the first X-ray interferometer. Soon, Deslattes [3] completed the count of the atoms in a natural silicon crystal and X-ray interferometry developed as a powerful tool in phase-contrast imaging [4] and, combined with optical interferometry, in linear and angular metrology at the atomic scale [5].

Johann Magnenus attempted to count atoms already in 1646 [6, 7]. He noted that the scent of a burned chickpea of incense filled a church of more than 7×10^8 times the volume of his nose. Eventually, with a guess of the atoms inside the nose, he estimated that 7.775×10^{17} is a lower bound to the number of atoms in the chickpea. What he did is essentially the same thing we do these days. Both amplify the atomic scale so that macro-scale detection is possible: Magnenus used diffusion and smell, we use crystallization and X-ray diffraction [8].

Since silicon can be grown as perfect, pure, and, nowadays, monoisotopic crystals, it was chosen as the Egidi's material. The spacing of its {220} planes gained a place among the fundamental physical constants of physics, became a link between the visible and the X- and γ-ray regions of the electromagnetic spectrum, and realised the metre at the nanometre and sub-nanometre scales.

Its measurement opened a broad field of metrological and science applications. In addition to the determination of the Avogadro constant, N_A [9] and, nowadays, to the realisation of the kilogram [10] it was instrumental to the determination of the h/m_n ratio [11, 12]. Combined with angle measurements, allowed the wavelength of X and γ rays to be referred to the metre [13–18], which resulted in improved measurements of the deuteron binding energy and neutron mass [16, 18] and in the most accurate test of the Planck–Einstein identity $h\nu = mc^2$ [19].

This article reviews the measurements of the spacing of the silicon {220} planes and describes the most critical

*Corresponding author, E-mail: e.massa@inrim.it

Springer

features of combined X-ray and optical interferometry. A summary of the values so far obtained is also given. The measurement procedure is described in detail, with emphasis on the critical points. Bottle-necks and clues of potential error sources that need further investigations are pointed out. Eventually, the possible evolutions of combined X-ray and optical interferometry as applied to the metrology of nano-structures and the manipulation of matter on the atomic scale are analysed.

2. Combined X-ray and Optical Interferometry

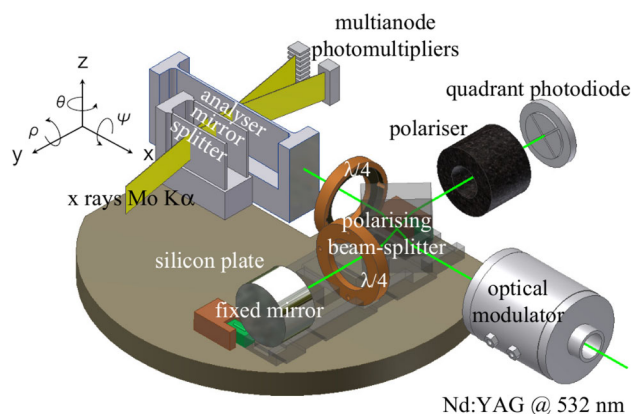A triple Laue interferometer is like a Mach–Zehnder one of visible optics. As shown in Figs. 1 and 2, it splits and recombines monoenergetic X-rays, coming from the 17 keV K_α transition of molybdenum, by a sequence of Laue diffractions in perfect Si crystals. The splitter, mirror, and analyser are cut in symmetric Laue geometry, where the {220} diffracting planes are perpendicular to their surfaces. When one of the interfering beams is phase-shifted, either by varying the optical length of one arm of the interferometer or by moving any one of the crystals orthogonally to the diffracting planes, interference fringes are observed in the output ports.

The measurement of the diffracting-plane spacing requires to split the analyser from the bulk of the X-ray interferometer. As it is displaced orthogonally to the {220} planes [20], a periodic variation of the transmitted and diffracted X-rays is observed, the period being the plane spacing, $d_{220} \approx 192$ pm.

To measure d_{220}, the front surface of the analyser is polished parallel to the diffracting plane to better than 10 µrad, and its displacement is measured by a laser interferometer having picometre sensitivity and accuracy. As shown in Fig. 3, the measurement equation is $d_{220} = m_\mathrm{opt}\lambda/(2n_x)$, where n_x is the number of X-ray fringes observed in m_opt optical orders of $\lambda/2$ period.

The X-ray and optical interferometers project the analyser motion on the normals to the diffracting planes and front mirror. Both projections must be equal to within 1 nm/m fractional error. Hence, the laser beam must be orthogonal to the front mirror to within 50 µrad and the motion straight and bisecting the above normals to within 0.1 mrad. Therefore, the transverse displacements must be controlled to within 10 nm/mm.

A different spacing of the diffracting planes of the fixed and movable crystals originates a pattern of vertical moiré fringes spaced by $\Lambda = d_{220}/\epsilon$, where ϵ is the strain of one crystal relative to the other. When integrating over 1 mm

Fig. 1 The INRIM's combined X-ray and optical interferometer. The first crystal splits the X-rays, which are recombined, via a mirror-like crystal, by the third. The interference fringes are imaged onto two multianode photomultipliers through stacks of eight NaI(Tl) scintillators. The analyser displacement is measured versus an auxiliary mirror mounted on the same silicon plate as the splitter–mirror pair. To achieve picometre resolution, the optical interferometer uses polarisation encoding (via a polarising beam-splitter and quarter wave-plates) and phase modulation
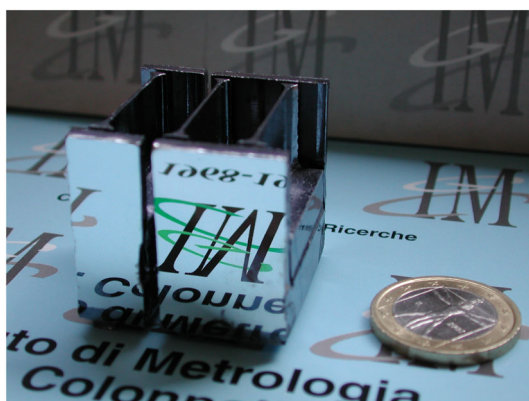

Fig. 2 The INRIM's MO*4 X-ray interferometer

Fig. 3 Measurement of the n_x/m_opt ratio. Green: optical fringes, red: X-ray fringes, n_x and m_opt: number of X-ray and optical fringes, respectively. The integer n_x/m_opt part—hypothetically, 10—is given in advance. After measuring the fractions of the X-ray fringes at the start and end of a $\lambda/2$ displacement, zero and 0.3, we obtain $n_x/m_\mathrm{opt} = 10.3$ and predict $n_x = 103$ over a $10 \times \lambda/2$ displacement. This procedure is repeated over longer and longer displacements

beam width, maximum contrast imposes strains less than 20 pm/mm.

Also, since the Si thermal expansion is about 2.5×10^{-6} 1/K, the crystal temperatures must be equal to within a few millikelvin. To ensure temperature uniformity and stability and to eliminate the adverse influence of the refractive index of air, the apparatus is hosted in a thermovacuum chamber.

2.1. X-ray Interferometer—Manufacturing

A good fringe contrast requires that the splitter and analyser thickness are equal and uniform to within a few micrometres and that the mirror thickness and the splitter-to-mirror and mirror-to-analyser gaps are identical to within the same tolerance. Furthermore, if the analyser movement combines with manufacturing errors, the interferometer geometry changes, which causes unwanted deviations of the fringe period from the spacing of the diffracting plane. Hence, the analyser surfaces must be orthogonal to the diffracting planes and the front surface to within 0.1 mrad.

The interferometer grinding by diamond tools can comply with these requirements; therefore, a subsequent chemically etching is necessary to remove the surface damage. If too little material is removed, lattice strains prevent the interferometer operation. If too much, the interferometer geometry degrades, and the fringe contrast is lost. Therefore, we must trade-off between no surface damage and accurate geometry. The optimum is re-machining with the finest grit size after a first etching. The final etching, for a depth of about 50 μm, is carried out by an electroless galvanic displacement mechanism in a water solution of $Cu(NO_3)_2$ ($\rho_{Cu(NO_3)_2} = 60$ g L^{-1}) and NH_4F ($\rho_{NH_4F} = 30$ g L^{-1}) [21]. In this process, the copper plates the silicon surface and, simultaneously, the oxidised silicon is removed by HF^- to form water-soluble silicates. The plating, which stops the silicon removal, is afterwards removed by a solution of iron chloride and etching requires continuously washing and dipping the interferometer in the two solutions. With respect to the usual HNO_3–HF etching, the advantages are the precise amount of Si removal (given by the number of cycles) and better geometrical control.

2.2. X-ray Interferometer—Alignment

The operation of a separate-crystal interferometer imposes stringent environmental and alignment requirements. After the separation, the fixed and movable crystals must be recombined in such a way the lattice atoms in one of the crystals face again those in the other. Also, they must be so spaced and aligned that the beams at the output ports overlap as perfectly as possible.

Owing to the limited photon-flux, about 10^3 photons s^{-1} mm^{-2}, the fringe-detection bandwidth does not exceed a few hertz. Therefore, the root-mean-square noise of the analyser position in the frequency band higher than, say, 10 Hz, must be less than a few picometres.

The Bragg-angle alignment of the analyser must match the Pendellösung oscillations of the interfering beams (one transmitted, the other reflected). With 1 mm thickness, to achieve the maximum contrast, the tolerance is 100 nrad. The analyser pitch-angle ρ ensures that its diffracting planes are parallel to those of the fixed crystal. A pitch rotation shifts the diffracting planes along the vertical and originates a pattern of horizontal moiré fringes spaced by $\Lambda = d_{220}/\rho$. To achieve the maximum contrast, integrating over a typical 10 mm beam height, the two crystals must be aligned to each other within a few nanoradian.

2.3. Measurement Procedure

To determine d_{220}, the same analyser displacement is measured with the optical and crystal-lattice rules. Next, we obtain the $\lambda/(2d_{220})$ ratio as the n_x/m_{opt} quotient of the numbers of X-ray, n_x, and optical, m_{opt}, periods, where the half-wavelength $\lambda/2$ is traceable to the metre.

With 1 pm sensitivity in the determination of the X-ray and optical fringe-fractions, the aimed 1 nm/m sensitivity can be obtained only by moving the analyser by no less than 1 mm. However, the time required for counting each X-ray period is unacceptable.

Instead, as shown in Fig. 3, we start from the known approximation $(n_x/m_{opt})_0 = 1385.9$ (@ $\lambda = 532$ nm and 20 °C), measure the residual fringe-fractions at the start and end of a $\lambda/2$ displacement, and predict the integer n_x part in a longer displacement. A least-squares estimator (see Fig. 4) determines the phases of the X-ray fringes at
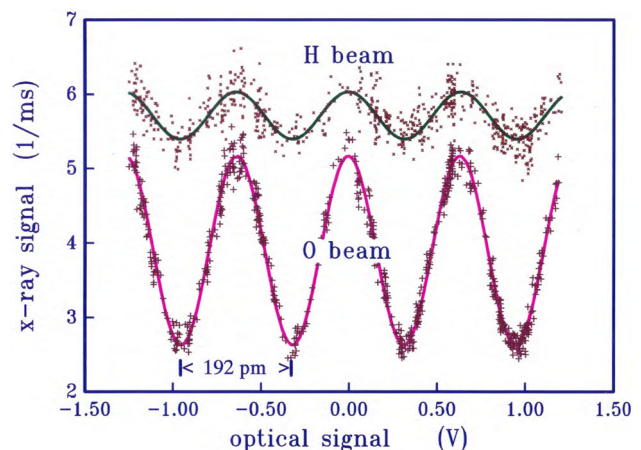

Fig. 4 X-ray fringe record versus the optical signal. The fringe phase at integer optical orders—set at the zero crossing of the optical signal—is estimated via best-fit sinusoidal models (solid lines)
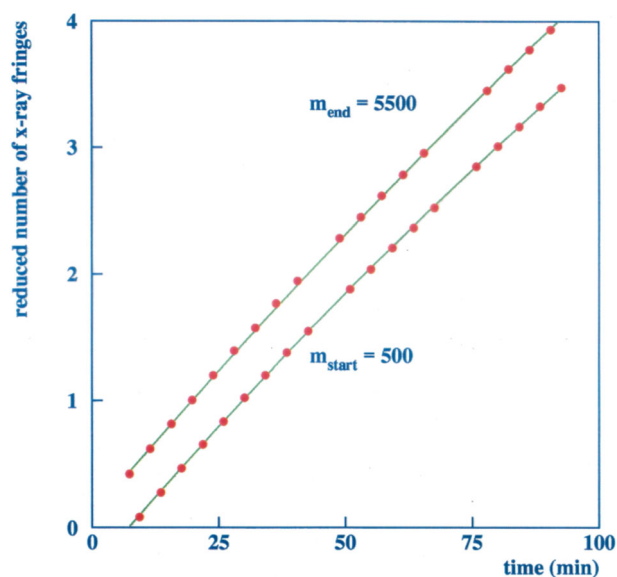
Fig. 5 Fractions of the X-ray fringes repeatedly measured at the optical orders 500 and 5500 (@ $\lambda = 633$ nm, about 1.6 mm). In the absence of any drift between the X-ray and optical interferometers, the two fractions would be constant and horizontal. The increasing gap is due to the lattice spacing drift because of 5 mK temperature variation

the displacement starts and ends optical orders, identified as the zero crossing of the demodulated signal. Iterations complete the measurement over increasing displacements.

As shown in Fig. 5, it is not possible to keep the drift between the X-ray and optical signals as small as wanted. Therefore, the analyser is moved repeatedly and rapidly back and forth and the signals are repeatedly sampled at the zero-crossings. Eventually, the fringe-fraction difference is obtained by demodulation.

Several systematic effects must be investigated, identified and corrected [22, 23]. Parasitic tilts of the analyser couple with the offset between the centroids of the X-rays and laser beam and cause Abbe-type errors. Unwanted transverse motions and imperfect alignment and diffraction of the laser beam change the projection angles of the analyser displacement on the measuring directions and cause cosine-type errors. Geometric errors and stress of the analyser surfaces cause extra phase delays of the crossing X-rays and diffracting-plane strains. Eventually, to correct for thermal expansion, the difference of the analyser temperature from the reference value must be kept as small as possible and measured to within sub-millikelvin accuracy.

Table 1 Natural Si: summary of measurement results at 22.500 °C (ITS-90 temperature scale) and 0 Pa

Lab	Crystal	Year	Δd_{220}/am Crystal	Δd_{220}/am Silicon	Reference
NBS	NBS73	1973	902.0(19)	–	[13, 25][a]
PTB	WASO4.2A	1981	563.0(12)	568.0(12)	[26][b]
IMGC	MO*4	1989	483.0(54)	501.0(54)	[27][b]
IMGC	MO*4	1994	551.0(5.0)	569.0(6.0)	[28, 29]
NMIJ	NRLM3	1997	587.0(10)	593.0(10)	[29, 30]
IMGC	MO*4	2004	551.3(3.4)	570.0(4.7)	[29, 31, 32]
NMIJ	NRLM3	2004	591.9(7.1)	597.6(7.3)	[29, 31, 32]
INRIM	NRLM3	2004	567.1(3.3)	572.9(3.7)	[29, 31, 32]
INRIM	WS5C (WASO04)	2007	571.0(3.2)	573.5(3.3)	[29][c]
INRIM	WASO4.2A	2007	570.5(3.3)	575.3(3.4)	[29]
INRIM	WASO4.2A	2007	571.5(1.8)	576.2(2.0)	[29]
INRIM	MO*4	2007	549.8(3.0)	568.4(4.5)	[29]
INRIM	MO*4	2008	550.8(1.2)	569.4(3.6)	[33]
INRIM	WASO4.2A	2009	569.1(1.0)	573.8(1.3)	[34]
INRIM	WS1A (WASO04)	2009	570.2(1.0)	572.7(1.3)	[35, 36][c]
INRIM	GAMS-I (WASO04)	2010	570.2(1.0)	572.7(1.3)	[36][c]

The Δd_{220} difference is to 192 015 000 am

[a] The temperature of the value given in [13] was $t_{68} = 25.0$ °C

[b] The temperature of the values given in [26, 27] was $t_{68} = 22.5$ °C

[c] WS5C, WS1A, and GAMS-I are different interferometers carved from the same WASO04 boule

3. Results

The {220} plane spacing of eight natural-Si interferometers (denoted NBS73, WASO4.2A, MO*4, NRLM3, WS5C, WS1A, GAMS-I) was determined using combined X-ray and optical interferometers. The results are shown Table 1 and Fig. 6. Since chemical impurities (mainly carbon, oxygen, and nitrogen) and point defects (vacancies and interstitials) strain the lattice, the measured values have been corrected to obtain the spacing of an impurity-free and crystallographically perfect crystal.

Soon, after the Bonse and Hart paper, three experiments started [37–39], but only the National Bureau of Standards (NBS, now National Institute of Standards and Technology—NIST) completed the measurement [13]. Eight years later, the Physikalisch-Technische Bundesanstalt (PTB) reported a more accurate value, which, however, differed from NBS's one much more than what expected from the associated uncertainties [26]. This inconsistency prompted further works at the Istituto di Metrologia "G. Colonnetti" (IMGC, now INRIM, Istituto Nazionale di Ricerca Metrologica) [27] and the National Research Laboratory of Metrology (NRLM, now NMIJ, National Metrology Institute of Japan) [30]. Today, only the INRIM's apparatus is operational.

Figure 7 shows how the measurement uncertainty reduced in time. Since the Deslattes' measurement in 1973, the quality of the interferometers improved (from natural Si [27] to hyper-pure Si [35] and enriched ^{28}Si [40]), the interferometer size and displacement increased (from a few micrometres [27] to 5 cm [33, 41]), the degrees of freedom electronically controlled extended (from one [27] to six [42]), differential wavefront sensing supplemented both X-ray and optical interferometry [43], and systematic effects were sought and investigated [23].
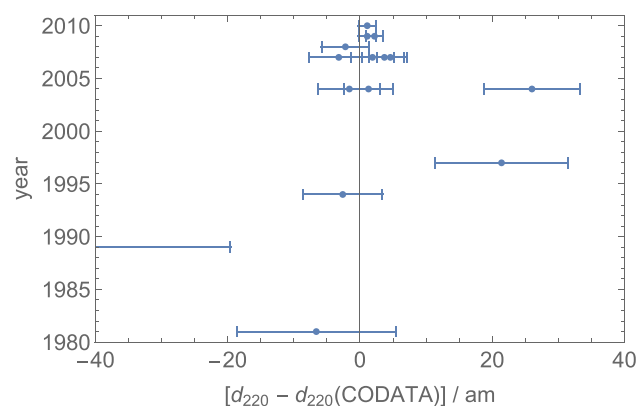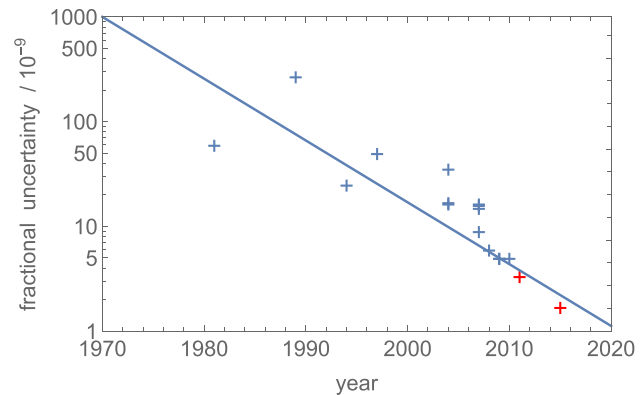

Fig. 7 Uncertainty improvement of the measurements of the {220} plane spacing of silicon crystals by combined X-ray and optical interferometry. Blue crosses: natural Si, red crosses: enriched ^{28}Si

The {220} plane spacing of silicon is relevant not only because of its, yesterday, relationship to the Avogadro and Planck constants and, today, the realisation of the kilogram, but also because it is instrumental to the measurements of the neutron mass [16, 18], the ratio between the Planck constant and neutron mass [11, 12], the test of the Planck–Einstein equation $h\nu = mc^2$ [19], and the absolute spectroscopy of X- and γ-ray wavelengths [13, 15–18].

The {220} plane spacing of the crystals used in these experiments was related to the values given in Table 1 by comparisons based on X-ray double crystal non-dispersive diffractometry. The results are given in Tables 2, 3, and 4.

Table 2 PTB fractional differences (expressed in nm/m) between the {220} plane spacing of samples of the given boules and a sample of the WASO04 one [44]

Si1	Si5	WASO4.2A
− 264(11)	+ 24(16)	− 1(6)
MO*4	NRLM3	WASO17
− 103(12)	− 23(6)	+ 22(10)

Samples of Si1 and Si5 were used to measure the h/m_n ratio [11, 12]

Table 3 NIST fractional differences (expressed in nm/m) between the {220} plane spacing of samples of the given boules and a sample of the WASO17 one [45]

MO*4	Si1	NRLM3
− 39(10)	− 235(10)	− 77(10)

A sample of Si1 was used to measure the h/m_n ratio [11, 12]

Table 4 NIST fractional differences (expressed in nm/m) between the {220} plane spacing of samples of the given boules and the ILL2.5 crystal [18]

WASO4.2A	MO*4	NRLM3
− 17(17)	− 86(10)	− 34(10)

Fig. 6 Results of the measurements of the {220} plane spacing of natural Si (see Table 1). The value recommended by the Committee on Data for Science and Technology (CODATA) is d_{220}(CODATA) = 192015571.6(32) am [24]

The comparisons used samples of the interferometer and sample-of-concern boules. Since the lattice parameter shows fractional variations of up to 10 nm/m over the boule volume (depending on the impurity level and concentration of point defects), variations of the samples' lattice parameter are possible. Improvements requires a direct (absolute) determinations of the lattice parameter values [36].

4. Measuring the Avogadro Constant

Since the crystallisation acts as a low-noise amplifier, the d_{220} measurement makes it possible to count the number of atoms in a silicon mole by exploiting their ordered arrangement. The measurement equation is

$$N_A = \frac{8M}{\rho a^3},\tag{1}$$

where M is the mean molar mass of a chemically pure and perfect mono-crystal, ρ is the density, $a = \sqrt{8}d_{220}$ is the lattice parameter, and 8 is the number of atoms in the cubic unit cell.

Deslattes completed the first count in 1974 [3]; further measurements soon followed [46–50]. At the end of the last century, the measurements came to a halt because of difficulties in the measurement of the natural silicon molar-mass [51].

In 2004, an international project (IAC—International Avogadro Coordination) got around this problem following an idea outlined by Zosi [52]. The participants combined resources and competence to grow a silicon crystal highly enriched by ^{28}Si [53], which made accurate molar-mass measurements possible by isotope dilution mass spectroscopy combined with multi-collector inductively coupled plasma mass spectrometry [54, 55].

To turn Egidi's idea into practice, two X-ray interferometers surrounded by two quasi-perfect 1 kg balls were cut out from the enriched ingot. The INRIM measured the lattice parameter of one of the interferometers to the utmost accuracy; the results are given in Table 5. To average the

Table 5 Enriched ^{28}Si crystal: summary of measurement results at 20.000 °C (ITS-90 temperature scale) and 0 Pa

Lab	Crystal	Year	Δd_{220}/am	Reference
INRIM	AVO28	2011	712.67(67)	[9, 40]
INRIM	AVO28	2015	711.98(34)	[9, 23]
INRIM	AVO28	2018	713.37(73)	[9][a]
INRIM	AVO28	2018	712.53(35)	[9][a]

The Δd_{220} difference is to 192 014 000 am

[a] The effects of the Si-surface stress and laser-beam diffraction on the 2011 and 2015 measured values have been reconsidered

Table 6 Enriched ^{28}Si: summary of measurement results of the Avogadro constant

Lab-year	Crystal	$N_A/10^{23}$ mol^{-1}	Reference
IAC-11	Si28-10-Pr11[a]	6.02214095(18)	[9, 65, 66]
IAC-15	Si28-10-Pr11[a]	6.02214070(12)	[9, 67]
IAC-17	Si28-23Pr11	6.022140526(70)	[9, 68]
NMIJ-17	Si28-10-Pr11[a]	6.02214078(15)	[9, 69]

[a] Short name: AVO28

measurement results over a representative part of the boule, particular care was taken to manufacture a big analyser crystal. The NIST and NMIJ verified the extrapolation of the interferometer lattice parameter to that of the balls by carrying out comparisons of samples taken all along the boule [56, 57].

To complete the N_A determination, the Bureau International des Poids et Mesures (BIPM), NMIJ, and PTB determined the ball mass [58], volume [59, 60], and chemical [61] and isotopic compositions [55, 62], and characterised their surfaces geometrically, chemically, and physically at the atomic scale [63]. The results, which are given in table 6, were used to stipulate the value of the Planck and Avogadro constants in the redefinition of the International System of Units [64].

5. Realising the Kilogram by Counting Si Atoms

Since the relative atomic masses are well measured, the masses of the silicon isotopes in terms of the Planck constant are accurately obtained from the measured quotients of the Planck constant and atom or particle masses, $h/m(e)$, $h/m(^{133}$Cs$)$, or $h/m(^{87}$Rb$)$.

Therefore, the mass of a pure, enriched, and perfect ^{28}Si single-crystal can be determined by counting its atoms [70]. In principle, one should take the mass defect associated with the binding energy of the atoms into account, but this correction is negligible at the present level of accuracy.

After measuring the lattice parameter and crystal volume V, the count is given by $N_{Si} = 8V/a^3$. Hence, for instance, the quotient of the crystal mass, m, and the Planck constant is

$$\frac{m}{h} = \frac{8V}{a^3}\frac{M(^{28}\text{Si})}{M(e)}\frac{m(e)}{h},\tag{2}$$

where $M(-)$ indicates the molar mass. The most convenient crystal shaping is like an optically polished nearly perfect ball, and the volume is obtained from an interferometric measurement of the average diameter.

Since silicon is never mono-isotopic, the amount-of-substance fraction, $f(^k$Si$)$, of each isotope ^{k}Si has to be measured and

$$M(\text{Si}) = \sum_{k=28}^{30} f(^{k}\text{Si})M(^{k}\text{Si}) \qquad (3)$$

must substitute for $M(^{28}\text{Si})$ in (2). A similar equation takes the chemical impurities and point defects (vacancies and interstitials) into account.

Eventually, the ball surface must be characterised to correct (2) for the mass of the oxide layer and the adsorbed or absorbed water and contaminants. By taking the uncertainty of the N_A values given in Table 6 into account, kilogram realisations to within 20 µg/kg fractional accuracy are at hands.

6. Outlook and Future Work

The Kibble balance and atom count realisations of the kilogram will be instrumental to future tests of the invariance of physics and technology across different disciplines and energies. They link status solidi physics (via the Josephson and quantum Hall effects) to, today, atomic physics (via optical spectroscopy and atom interferometry) or, tomorrow, nuclear physics (via γ spectroscopy and the mass defect in the capture of thermal neutrons by nuclei), as well as energy scales from meV to MeV.

Counting atoms is by no way limited to 1 kg, but, because of the fixed absolute accuracy of the diameter measurements and the worst surface-to-volume ratio, the count accuracy scales down linearly with the crystal size. For instance, the fractional accuracy of one gram realisation, by a silicon ball having about 1 cm diameter, is expected to be about 0.2 µg/g, which is still as good as or better than other realisations.

The main handicap of the atom count is the need for highly enriched crystals. However, the work with the ^{28}Si material made available a new way to determine the fractional abundances of each Si isotope by mass spectrometry and to calibrate the results to within the needed accuracy. Its extension and application to naturally occurring samples will be a decisive step towards widespread realisations.

Some points still need further investigations in combined X-ray and optical interferometry. Firstly, the surface stress makes the lattice parameter of X-ray interferometers different from that of the kilogram realisations. If the difference exceeded a few nm/m, it jeopardises the accuracy of the atom count. Numerical and experimental determinations of the surface stress are challenging [71, 72]. Phase-contrast topography of the induced lattice strains and lattice parameter measurements using a variable thickness interferometer are underway to work out the problem [73].

Secondly, wavefront distortions constitute a significant problem of optical interferometry. Wavefronts are never perfectly flat and any deformation changes with propagation. Therefore, the wavelength—the distance travelled by wavefronts during one oscillation period—is ill-defined, differs from that of the plane wave, and varies from one point to another. The relationship between the interference phase and the optical-path difference requires corrections that depend on the modal spectra of the interfering beams, interferometer operation, and phase detection technology [74–76].

In the third place, in optical heterodyne and polarisation encoding, the vector nature of the optical field implies geometrical contributions to the phase. Carrying polarizations through an interferometer is analogous to transport vectors on a sphere and leads to phase accumulations that appear as nonlinearities [77].

Lastly, an independent d_{220} measurement is still missing [78] and ultra-precision comparators for the lattice-plane spacing mapping and measurement are necessary [79].

Looking at the future of X-ray interferometry, it can effectively realise the metre at the nanoscale [80–82]. In the 1990s, the INRIM, National Physical Laboratory (NPL—UK), and PTB jointly built a combined optical and X-ray interferometry facility [5]. This one-dimensional machine integrates a monolithic X-ray interferometer and establishes traceability to the metre via the wavelength of a laser beam and the lattice parameter of silicon.

The measurement and control of centimetre one- and two-dimensional displacements with sub-atomic resolutions is a critical problem in the metrology of nano-structures and the manipulation of matter on the atomic scale. However, monolithic interferometers operate only over a few micrometres. The integration of a split bicrystal interferometer into atom-scale positioning and measuring machines, capable of integrating different probes, will underpin further developments.

Beyond these technological needs, science too is asking for even more demanding measurement and control capabilities, where X-ray interferometry and kindred technologies, researches, and developments can make the difference. Examples are the foreseen Laser Interferometer Space Antenna [83, 84], absolute X- and γ-ray spectrometry [77], separate-crystal neutron and X-ray interferometry [85, 86], and beam-line components for the fourth-generation synchrotrons [87].

Compliance with Ethical Standards

Conflict of interest The authors declare that they have no conflict of interest.

References

[1] C. Egidi, Nature **200**(10) (1965) 61

[2] U. Bonse, M. Hart, Applied Physics Letters **6**(8) (1965) 155

[3] R.D. Deslattes, A. Henins, H.A. Bowman, R.M. Schoonover, C.L. Carroll, I.L. Barnes, L.A. Machlan, L.J. Moore, W.R. Shields, Phys. Rev. Lett. **33** (1974) 463

[4] A. Momose, Nuclear Instruments and Methods in Physics Research Section A: Accelerators, Spectrometers, Detectors and Associated Equipment **352**(3) (1995) 622

[5] G. Basile, P. Becker, A. Bergamin, G. Cavagnero, A. Franks, K. Jackson, U. Kuetgens, G. Mana, E.W. Palmer, C.J. Robbie, M. Stedman, J. Stümpel, A. Yacoot, G. Zosi, Proceedings of the Royal Society of London. Series A: Mathematical, Physical and Engineering Sciences **456**(1995), 701 (2000)

[6] M. Quack, European Review **22**(S1) (2014) S50–S86

[7] J.C. Magnenus, *Democritus reviviscens*; Wyngaerden (1646) p. 207

[8] G. Mana, G. Zosi, La Rivista del Nuovo Cimento **18**(11) (1995) 1

[9] K. Fujii, E. Massa, H. Bettin, N. Kuramoto, G. Mana, Metrologia **55**(1) (2018) L1

[10] G. Mana, E. Massa, La Rivista del Nuovo Cimento **35**(7) (2012) 353

[11] E. Krueger, W. Nistler, W. Weirauch, Metrologia **35**(3) (1998) 203

[12] E. Krueger, W. Nistler, W. Weirauch, Metrologia **36**(2) (1999) 147

[13] R.D. Deslattes, A. Henins, Phys. Rev. Lett. **31** (1973) 972

[14] E.G. Kessler, R.D. Deslattes, A. Henins, W.C. Sauder, Phys. Rev. Lett. **40** (1978) 171

[15] E.G. Kessler, R.D. Deslattes, A. Henins, Phys. Rev. A **19** (1979) 215

[16] G.L. Greene, E.G. Kessler, R.D. Deslattes, H. Börner, Phys. Rev. Lett. **56** (1986) 819

[17] J. Härtwig, S. Grosswig, P. Becker, D. Windisch, Physica Status Solidi (A) **125**(1) (1991) 79

[18] J. E.G. Kessler, M. Dewey, R. Deslattes, A. Henins, H. Börner, M. Jentschel, C. Doll, H. Lehmann, Physics Letters A **255**(4) (1999) 221

[19] S. Rainville, J.K. Thompson, E.G. Myers, J.M. Brown, M.S. Dewey, E.G. Kessler, R.D. Deslattes, H.G. Boerner, M. Jentschel, P. Mutti, D.E. Pritchard, Nature **438**(12) (2005) 1096

[20] A. Bergamin, G. Cavagnero, G. Mana, E. Massa, G. Zosi, Measurement Science and Technology **10**(12) (1999) 1353

[21] E. Mendel, K-H Yang, Proceedings of the IEEE **57**(9) (1969) 1476

[22] G. Basile, A. Bergamin, G. Cavagnero, G. Mana, E. Vittone, G. Zosi, IEEE Transactions on Instrumentation and Measurement **40**(2) (1991) 98

[23] E. Massa, C.P. Sasso, G. Mana, C. Palmisano, Journal of Physical and Chemical Reference Data **44**(3) (2015) 031208

[24] E. Tiesinga, P.J. Mohr, D.B. Newell , B.N. Taylor, https://www.nist.gov/pml/fundamental-physical-constants (2018)

[25] P. Becker, G. Mana, Metrologia **31**(3) (1994) 203

[26] P. Becker, K. Dorenwendt, G. Ebeling, R. Lauer, W. Lucas, R. Probst, H.J. Rademacher, G. Reim, P. Seyfried, H. Siegert, Phys. Rev. Lett. **46** (1981) 1540

[27] G. Basile, A. Bergamin, G. Cavagnero, G. Mana, G. Zosi, IEEE Transactions on Instrumentation and Measurement **38**(2) (1989) 210

[28] G. Basile, A. Bergamin, G. Cavagnero, G. Mana, E. Vittone, G. Zosi, Phys. Rev. Lett. **72** (1994) 3133

[29] P. Becker, G. Cavagnero, U. Kuetgens, G. Mana, E. Massa, IEEE Transactions on Instrumentation and Measurement **56**(2) (2007) 230

[30] K. Nakayama, H. Fujimoto, IEEE Transactions on Instrumentation and Measurement **46**(2) (1997) 580

[31] G. Cavagnero, H. Fujimoto, G. Mana, E. Massa, K. Nakayama, G. Zosi, Metrologia **41**(1) (2004) 56

[32] G. Cavagnero, H. Fujimoto, G. Mana, E. Massa, K. Nakayama, G. Zosi, Metrologia **41**(6) (2004) 445

[33] L. Ferroglio, G. Mana, E. Massa, Opt. Express **16**(21) (2008) 16877

[34] E. Massa, G. Mana, U. Kuetgens, Metrologia **46**(3) (2009) 249

[35] E. Massa, G. Mana, U. Kuetgens, L. Ferroglio, New Journal of Physics **11**(5) (2009) 053013

[36] E. Massa, G. Mana, U. Kuetgens, L. Ferroglio, Journal of Applied Crystallography **43**(2) (2010) 293

[37] U. Bonse, E. teKaat, P. Spieker, in *Precision measurement and fundamental constants*, ed. by D.N. Langenberg, B.N. Taylor (Natl. Bur. Stand. Spec. Publ. 343) (1971), pp. 291–293

[38] I. Curtis, I. Morgan, M. Hart, A.D. Milne, in *Precision measurement and fundamental constants*, ed. by D.N. Langenberg, B.N. Taylor (Natl. Bur. Stand. Spec. Publ. 343) (1971), pp. 285–289

[39] R.D. Deslattes, in *Precision measurement and fundamental constants*, ed. by D.N. Langenberg, B.N. Taylor (Natl. Bur. Stand. Spec. Publ. 343) (1971), pp. 279–283

[40] E. Massa, G. Mana, U. Kuetgens, L. Ferroglio, Metrologia **48**(2) (2011) S37

[41] A. Bergamin, G. Cavagnero, L. Cordiali, G. Mana, G. Zosi, IEEE Transactions on Instrumentation and Measurement **46**(2) (1997) 576

[42] A. Bergamin, G. Cavagnero, G. Durando, G. Mana, E. Massa, Measurement Science and Technology **14**(6) (2003) 717

[43] A. Bergamin, G. Cavagnero, G. Mana, Review of Scientific Instruments **64**(11) (1993) 3076

[44] J. Martin, U. Kuetgens, J. Stuempel, P. Becker, Metrologia **35**(6) (1998) 811

[45] E.G. Kessler, J.E. Schweppe, R.D. Deslattes, IEEE Transactions on Instrumentation and Measurement **46**(2) (1997) 551

[46] P. Sevfried, P. Becker, A. Kozdon, F. Lüdicke, F. Spieweck, J. Stümpel, H. Wagenbreth, D. Windisch, P. De Bièvre, H.H. Ku, G. Lenaers, T.J. Murphy, H.S. Peiser, S. Valkiers, Zeitschrift für Physik B Condensed Matter **87**(3) (1992) 289

[47] G. Basile, P. Becker, A. Bergamin, H. Bettin, G. Cavagnero, P. De Bièvre, U. Kutgens, G. Mana, M. Mosca, B. Pajot, R. Panciera, W. Pasin, S. Pettorruso, A. Peuto, A. Sacconi, J. Stumpel, S. Valkiers, E. Vittone, G. Zosi, IEEE Transactions on Instrumentation and Measurement **44**(2) (1995) 538

[48] P. De Bièvre, S. Valkiers, S. Peiser, P. Becker, F. Ludicke, F. Spieweck, J. Stuempel, IEEE Transactions on Instrumentation and Measurement **44**(2) (1995) 530

[49] K. Fujii, M. Tanaka, Y. Nezu, K. Nakayama, H. Fujimoto, P.D. Bièvre, S. Valkiers, Metrologia **36**(5) (1999) 455

[50] K. Fujii, A. Waseda, N. Kuramoto, S. Mizushima, P. Becker, H. Bettin, A. Nicolaus, U. Kuetgens, S. Valkiers, P. Taylor, P. De Bièvre, G. Mana, E. Massa, R. Matyi, E.G. Kessler, M. Hanke, IEEE Transactions on Instrumentation and Measurement **54**(2) (2005) 854

[51] S. Valkiers, G. Mana, K. Fujii, P. Becker, Metrologia **48**(2) (2011) S26

[52] G. Zosi, Lettere al Nuovo Cimento **38** (1983) 577

[53] P. Becker, D. Schiel, H.J. Pohl, A.K. Kaliteevski, O.N. Godisov, M.F. Churbanov, G.G. Devyatykh, A.V. Gusev, A.D. Bulanov, S.A. Adamchik, V.A. Gavva, I.D. Kovalev, N.V. Abrosimov, B. Hallmann-Seiffert, H. Riemann, S. Valkiers, P. Taylor, P.D. Bièvre, E.M. Dianov, Measurement Science and Technology **17**(7) (2006) 1854

[54] G. Mana, O. Rienitz, A. Pramann, Metrologia **47**(4) (2010) 460

[55] A. Pramann, O. Rienitz, D. Schiel, J. Schlote, B. Güttler, S. Valkiers, Metrologia **48**(2) (2011) S20

[56] E. Massa, G. Mana, L. Ferroglio, E.G. Kessler, D. Schiel, S. Zakel, Metrologia **48**(2) (2011) S44

[57] H. Fujimoto, A. Waseda, X.W. Zhang, Metrologia **48**(2) (2011) S55

[58] A. Picard, P. Barat, M. Borys, M. Firlus, S. Mizushima, Metrologia **48**(2) (2011) S112

[59] N. Kuramoto, K. Fujii, K. Yamazawa, Metrologia **48**(2) (2011) S83

[60] G. Bartl, H. Bettin, M. Krystek, T. Mai, A. Nicolaus, A. Peter, Metrologia **48**(2) (2011) S96

[61] S. Zakel, S. Wundrack, H. Niemann, O. Rienitz, D. Schiel, Metrologia **48**(2) (2011) S14

[62] E. Bulska, M.N. Drozdov, G. Mana, A. Pramann, O. Rienitz, P. Sennikov, S. Valkiers, Metrologia **48**(2) (2011) S32

[63] I. Busch, Y. Azuma, H. Bettin, L. Cibik, P. Fuchs, K. Fujii, M. Krumrey, U. Kuetgens, N. Kuramoto, S. Mizushima, Metrologia **48**(2) (2011) S62

[64] P.J. Mohr, D.B. Newell, B.N. Taylor, E. Tiesinga, Metrologia **55**(1) (2018) 125

[65] B. Andreas, Y. Azuma, G. Bartl, P. Becker, H. Bettin, M. Borys, I. Busch, M. Gray, P. Fuchs, K. Fujii, H. Fujimoto, E. Kessler, M. Krumrey, U. Kuetgens, N. Kuramoto, G. Mana, P. Manson, E. Massa, S. Mizushima, A. Nicolaus, A. Picard, A. Pramann, O. Rienitz, D. Schiel, S. Valkiers, A. Waseda, Phys. Rev. Lett. **106** (2011) 030801

[66] B. Andreas, Y. Azuma, G. Bartl, P. Becker, H. Bettin, M. Borys, I. Busch, P. Fuchs, K. Fujii, H. Fujimoto, E. Kessler, M. Krumrey, U. Kuetgens, N. Kuramoto, G. Mana, E. Massa, S. Mizushima, A. Nicolaus, A. Picard, A. Pramann, O. Rienitz, D. Schiel, S. Valkiers, A. Waseda, S. Zakel, Metrologia **48**(2) (2011) S1

[67] Y. Azuma, P. Barat, G. Bartl, H. Bettin, M. Borys, I. Busch, L. Cibik, G. D'Agostino, K. Fujii, H. Fujimoto, A. Hioki, M. Krumrey, U. Kuetgens, N. Kuramoto, G. Mana, E. Massa, R. Meeß, S. Mizushima, T. Narukawa, A. Nicolaus, A. Pramann, S.A. Rabb, O. Rienitz, C. Sasso, M. Stock, R.D. Vocke, A. Waseda, S. Wundrack, S. Zakel, Metrologia **52**(2) (2015) 360

[68] G. Bartl, P. Becker, B. Beckhoff, H. Bettin, E. Beyer, M. Borys, I. Busch, L. Cibik, G. D'Agostino, E. Darlatt, M.D. Luzio, K. Fujii, H. Fujimoto, K. Fujita, M. Kolbe, M. Krumrey, N. Kuramoto, E. Massa, M. Mecke, S. Mizushima, M. Müller, T. Narukawa, A. Nicolaus, A. Pramann, D. Rauch, O. Rienitz, C.P. Sasso, A. Stopic, R. Stosch, A. Waseda, S. Wundrack, L. Zhang, X.W. Zhang, Metrologia **54**(5) (2017) 693

[69] N. Kuramoto, S. Mizushima, L. Zhang, K. Fujita, Y. Azuma, A. Kurokawa, S. Okubo, H. Inaba, K. Fujii, Metrologia **54**(5) (2017) 716

[70] K. Fujii, H. Bettin, P. Becker, E. Massa, O. Rienitz, A. Pramann, A. Nicolaus, N. Kuramoto, I. Busch, M. Borys, Metrologia **53**(5) (2016) A19

[71] C. Melis, L. Colombo, G. Mana, Metrologia **52**(2) (2015) 214

[72] C. Melis, S. Giordano, L. Colombo, G. Mana, Metrologia **53**(6) (2016) 1339

[73] E. Massa, C.P. Sasso, M. Fretto, L. Martino, G. Mana, Journal of Applied Crystallography **53**(5) (2020) 1195

[74] G. Mana, E. Massa, C.P. Sasso, Metrologia **55**(4) (2018) 535

[75] G. Mana, E. Massa, C.P. Sasso, Metrologia **55**(2) (2018) 222

[76] G. Mana, C.P. Sasso, Metrologia **56**(5) (2019) 055004

[77] E. Massa, G. Mana, J. Krempel, M. Jentschel, Opt. Express **21**(22) (2013) 27119

[78] B. Andreas, U. Kuetgens, Measurement Science and Technology **31**(11) (2020) 115005

[79] J. Yang, T. Li, Y. Zhu, X. Zhang, A. Waseda, H. Fujimoto, Journal of Synchrotron Radiation **27**(3) (2020) 577

[80] The international system of units (SI) appendix 2: practical realization of the definition of some important units. Bureau International des Poids et Mesures (2019)

[81] M. Aketagawa, Y. Ikeda, N. Tanyarat, M. Ishige, Measurement Science and Technology **18**(2) (2007) 503

[82] M. Çelik, R. Hamid, U. Kuetgens, A. Yacoot, Measurement Science and Technology **23**(8) (2012) 085901

[83] M. Tröbs, L. d'Arcio, S. Barke, J. Bogenstahl, in *International conference on space optics and ICSO 2012*, vol. 10564, ed. by B. Cugny, E. Armandillo, N. Karafolas. International Society for Optics and Photonics (SPIE), vol. 10564 (2019), pp. 965–975

[84] C.P. Sasso, G. Mana, S. Mottini, Opt. Express **27**(12) (2019) 16855

[85] A. Yoneyama, A. Momose, E. Seya, K. Hirano, T. Takeda, Y. Itai, Review of Scientific Instruments **70**(12) (1999) 4582

[86] K. Tamasaku, M. Yabashi, T. Ishikawa, Phys. Rev. Lett. **88** (2002) 044801

[87] M. Agåker, F. Mueller, B. Norsk Jensen, K. Åhnberg, P. Sjöblom, J. Deiwiks, H. Henniger, R. Pärna, J. Knudsen, B. Thiagarajan, C. Såthe, Journal of Synchrotron Radiation **27**(2) (2020) 262